

DYNAMIC MODELING AND STABILITY ANALYSIS OF A NONLINEAR SYSTEM WITH PRIMARY RESONANCE

Romes. A. Borges¹, Marcos N. Rabelo¹, Alcione B. Purcina¹, Marcos L. Henrique²

¹Federal University of Catalão– Mathematics and Technology Institute – School of Industrial Mathematics, CEP 75704-020, Catalão, GO, Brazil.

²Interdisciplinary Nucleus of Exact Sciences and Technological Innovation, Federal University of Pernambuco, Campus Agreste, Caruaru-PE, CEP. 55002-971, Brazil.

Corresponding author: Romes A. Borges - romes@ufg.br

Abstract

In recent years, there has been growing interest in the study of nonlinear phenomena. This is due to the modernization of structures related to the need of using lighter, more resistant and flexible materials. Thus, this work aims to study the behavior of a mechanical system with two degrees of freedom with nonlinear characteristics in primary resonance. The structure consists of the main system connected to a secondary system to act as a Nonlinear Dynamic Vibration Absorber, which partially or fully absorbs the vibrational energy of the system. The numerical solutions of the problem are obtained using the Runge-Kutta methods of the 4th order and approximate analytical solutions are obtained using the Multiple Scales Method. Then, the approximation error between the two solutions is analyzed.

Using the aforementioned perturbation method, the responses for the ordinary differential equations of the first order can be determined, which describe the modulation amplitudes and phases. Thus, the solution in steady state and the stability are studied using the frequency response. Furthermore, the behavior of the main system and the absorber are investigated through numerical simulations, such as responses in the time domain, phase planes and Poincaré map; which shows that the system displays periodic, quasi-periodic and chaotic movements. The dynamic behavior of the system is analyzed using the Lyapunov exponent and the bifurcation diagram is presented to better summarize all the possible behaviors as the force amplitude varies. In general, the main characteristics of a dynamic system that experiences the chaotic response will be identified.

Keywords: nonlinear mechanical systems, primary resonances, multiple scales method, Lyapunov exponent, Poincaré map, stability analysis and chaos

1 Introduction

The decrease in vibration levels in the response of a system is vitally important to have a reliable and efficient design as these vibrations are undesirable phenomena that may cause damage, failure, and sometimes destruction of machines and structures. According to Sayed [1], the vibration analysis of mechanical systems can provide information and improve a design in terms of quality, durability and productivity. They considered a two degree of freedom vibration system including quadratic and cubic nonlinearities subjected to external and parametric excitation forces and solved it using the multiple scale

perturbation method. All possible resonance cases are extracted; however, the stability of the system is investigated at one of the worst resonance cases, confirmed numerically, which is the simultaneous primary, principal parametric and internal resonance. The system is studied numerically for selected values of different parameters. The numerical simulations show that the system exhibits periodic motions and chaotic motions, and that the vibration of the main system can be controlled applying a nonlinear absorber. Thus, there is growing interest in tools to attenuate unwanted vibrations in various types of systems. One of the most effective ways to attenuate unwanted vibrations in a given structure is through Dynamic Vibration Absorbers [2]. A classic DVA consists of a mass coupled by means of a spring and a damper to a given system, obtaining a new degree of freedom. The system is then tuned to vibrate at higher amplitudes, absorbing thereby partially or fully vibratory energy in the coupling point, see [3]. The DVAs may have linear or nonlinear characteristics. However, in recent years, there has been increasing interest in studying DVAs with nonlinear characteristics, due to their greater robustness when compared to the linear absorber, based on the fact that linear DVA operates satisfactorily only in its tuning frequency [4].

In recent years, more attention has been paid to the study of nonlinear phenomena due to the modernization of structures, thus there are various studies concerning different models of continuous systems. [5], [6]. However, methods for analyzing nonlinear systems, the opposite of linear, are far less known; some are only found partially developed and analysing the equations that model a given problem are difficult to apply. Nonlinearities offer greater variability in the solutions. Therefore, it is necessary to formulate mechanisms to study and understand the characteristics of nonlinear phenomenon, emphasizing the chaos [7], [8].

One of the particularities of systems which show chaos is the high sensitivity to the initial conditions, that is, solutions with near initial conditions have a completely different behavior [9].

Differential equations that describe vibration systems are usually nonlinear and not always is it possible to obtain an analytical solution. However, often an approximate solution can be obtained. One of the most efficient ways of handling nonlinear phenomena is the perturbation theory, which is defined by interactive methods that has the purpose of obtaining approximate solutions involving a suitable choice of perturbation parameters. The only drawback of the theory is that it provides good results only for small displacements [10]. Still with respect to non-linearity, [11] studied the stability on a system of a two degree of freedom for various time delayed values to confirm its influence on the attenuation of vibrations.

Among the perturbation methods is the multiple scales method. The basic idea of this method is to achieve the expansion of the solution representing the response as a function of multiple independent variables or multiple scales [8]. Due to their wide range of applications, perturbation methods have been used to analyze vibration phenomena of various types of problems in engineering. In particular, bifurcation and stability problems have been solved by means of perturbation techniques. We will briefly review the state of art involving these techniques and how they can be applied in solutions to problems regarding chaotic behavior.

In [12], a numerical method is presented to analyze the bifurcation due to both lateral and torsional vibrations in rotating systems. A nonlinear model with three degrees of freedom is obtained from the Hamiltonian formulation. Using a standard procedure from classical mechanics, the authors showed that the dynamic of the system is described using nonlinear differential equations. From this model and using

the linearized matrix of the system, the stability of the equilibrium points and the linear normal modes are analyzed. The bifurcation of periodic orbits is investigated using a computing algorithm of the nonlinear normal modes adopting the multiple shooting technique and the pseudo ArcLength continuation method.

The Routh-Hurwitz stability criterion is used to investigate the absolute stability of dynamic systems. Edward John Routh (1831-1907) established the first criterion for a polynomial to have roots (solutions) with a negative real part. However, Adolf Hurwitz (1859-1919) classified this as a necessary condition, but not sufficient and developed the Hurwitz matrix or H matrix, built through the coefficients of the polynomial. Thus, the criterion established that, besides the polynomial having all its positive coefficients, all the determinants of the matrix also had to be positive. [7].

Passive suppression mechanism of the vortex-induced vibration in solids, based on nonlinear elements and a nonlinear energy sink are investigated in [13]. A van der Pol oscillator is used to model a load-induced flow and in the main frame a structure is coupled that works as a nonlinear energy sink. Based on the equations of motion, the analysis performed indicated that the mass and frequency of the nonlinear energy sink showed significant effects in reducing the vibration response [13].

One of the most important criteria among those used to define chaos in dynamic systems is the Lyapunov exponent that measures the exponential average rate of divergence or convergence of phase space trajectories. Thus, the dynamic behavior of a system can be provided through signs of the Lyapunov exponents, which indicate the presence of fixed points, periodic movements, almost periodic and chaos [5]. There is also interest in experimentally studying nonlinear phenomena. An interesting study, [14], involves the experimental study of resonance of a discrete structure with forced oscillations.

Chaotic responses in the study of vibrations in beams attached to non-linear springs, which are in turn bound to a foundation, are investigated in [15]. In this case, the equations of motion are obtained and used to produce the Poincaré section in phase space. Together with the Lyapunov exponent, these techniques are used to study the chaotic behavior of the frequency response of the system. Resonance conditions and the existence of homoclinic orbits are also analyzed.

According to [7], another useful procedure for analyzing chaotic behavior is the bifurcation diagram. In general, bifurcation is understood as a qualitative shift in the nature of the dynamical system behavior because of the variation of the parameters. The bifurcation theory is usually developed in two ways: local bifurcations, which treat bifurcations in a limited region of the phase space, and global bifurcations that represent a qualitative change in the structure of orbits in a region of phase space.

In [16], the problem of chaotic motion of a nonlinear elastic beam axially compressed and subject to a transversal load was considered. The authors assumed that the damping force, as well as the material used to manufacture the element were nonlinear in nature. From there, the non-linear governing equation was obtained, as well as the corresponding dynamic system using the non-linear Galerkin method. The Melnikov's method was used to study the existence of homoclinic orbits. According to the authors, the results showed suitable choices of loaded parameters yielding to chaotic behavior of the vibration response. [17] studied the nonlinear dynamics of a two-degree-of-freedom vibration system with nonlinear damping and nonlinear spring. The bifurcation diagram, the Poincaré map and amplitude–frequency spectrum are analyzed to identify the periodic motion, quasiperiodic motion and chaotic motion of the system. It is worth

mentioning that according to the authors the numerical simulation shows that the effect of reduction of the vibration amplitude can be obtained by properly selecting the values of nonlinear dampers, nonlinear spring stiffness and the range of exciting frequency.

Another very interesting study was that of chaotic dynamics of a Duffing system with softening stiffness, subject to periodic external forces with multiple frequencies [18]. The authors pointed out that the mechanism that generates chaos is the transversality of homoclinic orbits when considered in the torus. Using the concept of stable and unstable manifolds, the authors obtained the Melnikov's function, which in turn is used to determine the existence of homoclinic orbits. From the existence of homoclinic orbits, the authors estimate both the Poincaré map and a parameter region where the chaotic dynamics may occur.

Chaotic phenomena are a behavior that rise in dynamical systems and their causes are due to many factors such as the number of degrees of freedom, the geometry of the problem and movement constraint among others. In recent years, the study of chaotic dynamics has attracted the attention of researchers in the field, due to its unpredictability in relation to the analysis and the effects that nonlinearities can cause in the stability of the system [19].

In this paper, our main aim is to study the emergence of chaotic behavior of the dynamic vibration absorber subject to nonlinear elements in the stiffness. It is assumed that the system operates in primary resonance. From the method of multiple scale techniques [20], an approximate analytical solution is given and compared numerically through four Runge Kutta methods [21]. In addition, the Routh-Hurwitz is used to establish a parameter region of stability. The chaotic behavior and existence of bifurcation solutions is analyzed through Poincaré mapping and Lyapunov exponent methods. The article finishes with a numerical analysis using Matlab® software.

2 Modeling a discrete system

In this section, our main concern is the vibratory system of two degrees of freedom where the concept of Nonlinear Dynamic Vibration Absorber (nDVA) is introduced [22]. The main aim of the device (absorber) is to attenuate the vibration levels of the main system, as can be seen in Fig. 1.

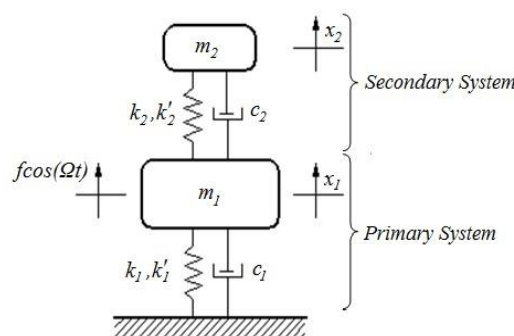


Figure 1: Discrete mechanical system.

By applying Newton's second law in the two masses separately, we have the following set of motion equations:

$$m_1 \ddot{x}_1 + k_1 x_1 + k_1' x_1^3 + c_1 \dot{x}_1 - k_2 (x_2 - x_1) - c_2 (\dot{x}_2 - \dot{x}_1) = f \cos(\Omega t) \tag{1}$$

$$m_2 \ddot{x}_2 + k_2(x_2 - x_1) + k_2'(x_2 - x_1)^3 + c_2(\dot{x}_2 - \dot{x}_1) = 0 \tag{2}$$

$$\ddot{x}_1 + \omega_1^2 x_1 + \epsilon \alpha_1 x_1^3 + \epsilon \xi_1 \dot{x}_1 + \epsilon \alpha_2 x_2 - \epsilon \alpha_3 (x_2 - x_1)^3 + \epsilon \xi_2 (\dot{x}_1 - \dot{x}_2) = \epsilon f \cos(\Omega t) \tag{3}$$

$$\ddot{x}_2 + \omega_2^2(x_2 - x_1) + \epsilon \beta_1(x_2 - x_1)^3 + \epsilon \xi_3(\dot{x}_2 - \dot{x}_1) = 0 \text{ where} \tag{4}$$

$$\omega_{12} = \frac{k+k'}{m_1}, \omega_{22} = \frac{k}{m_2}, \alpha_1 = \frac{k'}{m_1}, \alpha_2 = \frac{k}{m_1}, \alpha_3 = \frac{k'}{m_1}, m_1 \quad m_2 \quad m_1 \quad m_1 \quad m_1 \tag{5}$$

$$\xi_1 = \frac{c}{m_1}, \xi_2 = \frac{c}{m_2}, \xi_3 = \frac{c}{m_2}, \beta_1 = \frac{k'}{m_2}, f = \frac{f}{m_1}, \tag{6}$$

c_1	main system	0.1	Ns/m
c_2	Linear absorber damping constant	0.08	Ns/m

This vibrating system consists of springs (k_1, k_2') with nonlinear characteristics, which are assumed to be sufficiently weak. An external force $f(t) = \cos(\Omega t)$ excites the main m_1 mass.

We can rewrite Eq. (1) and (2) in the following way:

$$m_1 \ddot{x}_1 + m_1 \omega_1^2 x_1 + \epsilon \alpha_1 x_1^3 + \epsilon \xi_1 \dot{x}_1 + \epsilon \alpha_2 x_2 - \epsilon \alpha_3 (x_2 - x_1)^3 + \epsilon \xi_2 (\dot{x}_1 - \dot{x}_2) = \epsilon f \cos(\Omega t)$$

and $\epsilon \ll 1$ is used to indicate values with a small order of magnitude.

Table 1 lists the parameter values of the main system and the absorber.

Table 1: Parameter Values of the System

Symbol	Variable	Value	Unit
m_1	Mass of main system	10	kg
m_2	Absorber mass	0.8	kg
k_1	Linear stiffness of the main system	44	N/m
k_1'	Nonlinear stiffness of the main system	8	N/m ³
k_2	Linear absorber stiffness	2	N/m ³
k_2'	Nonlinear absorber stiffness	0.5	N/m ³

Linear damping constant of the

3 The multiple scales method applied to a nonlinear mechanical system

In this section, our aim is to use the multiple scale technique according to [23] to uniformly approximate the solution of Eqs. (3) and (4). In order to perform the calculation, we will consider the expansion of the solution with two terms

$$x_1(t,;\varepsilon) = x_{10}(T_0, T_1) + \varepsilon x_{11}(T_0, T_1) \tag{7}$$

$$x_2(t,;\varepsilon) = x_{12}(T_0, T_1) + \varepsilon x_{21}(T_0, T_1) \tag{8}$$

where $T_0 = t$ and $T_1 = \varepsilon t$, represent the slow and fast scale, respectively, of the time. As can

be seen, the expansion is performed until $O(\varepsilon^2)$, and $x_j, j = 1, 2$, are functions to be determined.

Taking into account the previous comments and using the chain of rules, the first and second order derivatives of x in relation to time should be expressed in terms of partial derivatives, relatively the T_n such that,

$$\frac{dx}{dt} = D_0 + \varepsilon D_1, \tag{9}$$

$$\frac{d^2x}{dt^2} = 2\varepsilon D_0 D_1, \tag{10}$$

$D_0 +$

where $D_n = \frac{\partial}{\partial T_n}$ ($n = 0, 1, \dots$) are differential operators.

$O(\varepsilon^2)$

Substituting Eqs. (7) and (8) in Eqs. (3) and (4) and separating the terms with power of the same order, we obtain the following set of equations:

Order $O(\varepsilon^0)$:

$$(D_0^2 + \omega_1^2)x_{10} = 0 \tag{11}$$

$$(D_0^2 + \omega_2^2)x_{20} = \omega_2^2 x_{10} \tag{12}$$

• Order $O(\varepsilon^1)$:

$$(-D_0^2 + \omega_1^2)x_{11} - 2D_0 D_1 x_{10} - D_1^2 x_{10} - D_0 D_1 x_{20} + D_1^2 x_{20} + 3D_0 D_1 (x_{20} - x_{10}) = 0 \tag{13}$$

$$(D_0^2 + \omega_2^2)x_{21} = -2D_0 D_1 x_{20} + \omega_2^2 x_{11} - D_1^2 (x_{20} - x_{10}) - 3D_0 D_1 (x_{20} - x_{10}) \tag{14}$$

The general solutions of Eqs. (11) and (12) can be expressed in the following ways:

$$x_{10} = Ae^{i\Gamma_1 T_0} + cc \tag{15}$$

$$x_{20} = Be^{i\Gamma_2 T_0} + \Gamma_1 Ae^{i\Gamma_1 T_0} + cc \tag{16}$$

where $\Gamma_j = \frac{\omega_j^2}{\omega_2^2 - \omega_1^2}$, A and B are unknown functions of T_1 and which can be calculated from

$$\omega_2^2 - \omega_1^2$$

the elimination of secular terms at the right hand side of the equations. The particular solutions of Eqs. (13) and (14) are given by:

$$x_{11} = Ce^{i\omega_1 T_0} + U_1 e^{i\Omega T_0} + H_1 e^{3i\omega_1 T_0} + H_2 e^{i\omega_2 T_0} + H_3 e^{3i\omega_2 T_0} + H_4 e^{i(2\omega_1 + \omega_2) T_0} + H_5 e^{i(2\omega_1 - \omega_2) T_0} + H_6 e^{i(\omega_1 + 2\omega_2) T_0} + H_7 e^{i(\omega_1 - 2\omega_2) T_0} + cc \tag{17}$$

$$x_{21} = De^{i\omega_2 T_0} + U_2 e^{i\Omega T_0} + H_8 e^{i\omega_1 T_0} + H_9 e^{3i\omega_1 T_0} + H_{10} e^{3i\omega_2 T_0} + H_{11} e^{i(2\omega_1 + \omega_2) T_0} + H_{12} e^{i(2\omega_1 - \omega_2) T_0} + H_{13} e^{i(\omega_1 + 2\omega_2) T_0} + H_{14} e^{i(\omega_1 - 2\omega_2) T_0} + cc \tag{18}$$

where $C, D, U_j, j = 1, 2$, and $H_i = 1, \dots, 14$, are complex functions in T_1 .

The general solution of x_1 and x_2 until the first order approximation is given by:

$$x_1 = x_{10} + \epsilon x_{11} \tag{19}$$

$$x_2 = x_{20} + \epsilon x_{21} \tag{20}$$

3.1 Evaluation of the response obtained by the Multiple Scale Method

The search for precisely approximate solutions of an equation can be performed in two ways: Numerical Method (Fourth-Order Runge-Kutta Method) and Analytical Methods (Multiple Scale Method). An analytical approach is obtained when a parameter of the problem is small, hence the name [10], [24].

After the solution has been calculated analytically, it can be observed to what extent the numerical solution of the system in question can be approximated

In order to evaluate the efficiency of the analytical solution through the Multiple Scale Method and the numerical solution (fourth order Runge-Kutta), the relation between these two solutions is presented in Figure 2 (a) and (b). Considering this, it can be observed that the perturbation method used is satisfactory to represent the response of the presented non-linear system. The values are listed in Table 1, presented in the previous section.

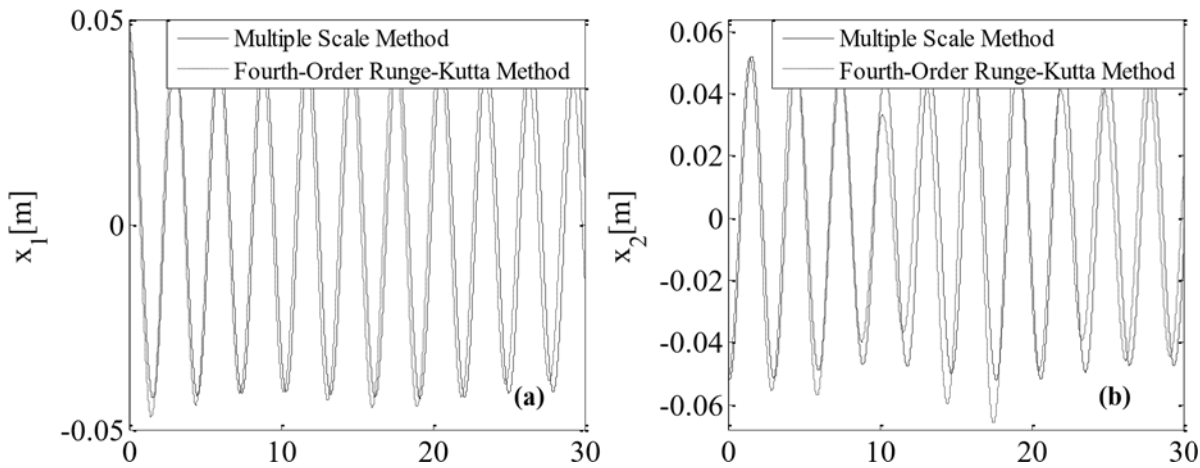


Figure 2: main system (a) and absorber (b): numerical solution - equation (3) and (4) and analytical solution - equations (19) and (20).

This shows that the general solution obtained by the perturbation method, to the first order approximation is sufficiently close to the numerical solution for the nonlinear system, although it presents some discrepancy points of the oscillation amplitude. For better accuracy of the analytical solution, generally terms of higher orders have to be considered in the expansion [11], [25].

4 Study of the stability in the mechanical system

The stability of the vibratory system of two degrees of freedom, with damping, is investigated for the case of the primary resonance, i.e., in which the frequency of the external excitation Ω is very close to the natural frequency ω_1 . As usual, instead of using the excitation frequency Ω as a parameter, a tuning parameter σ is introduced, such that [26]:

$$\Omega = \omega_1 + \varepsilon\sigma, \tag{21}$$

Substituting Eq. (21) in Eqs. (13) and (14) and eliminating the secular terms leads to the following conditions of solvability:

$$2i\omega_1 D_1 A = [-\xi_1 i \omega_1 + \alpha_2 \Gamma_1 + \xi_2 i \omega_1 (\Gamma_1 - 1)] A - 3[\alpha_1 \alpha_3 (\Gamma_1 - 1)^3] A^2 + 6\alpha_3 (\Gamma_1 - 1) A B B + 2f e^{i\sigma t} \tag{22}$$

$$\omega_2^2 [6\alpha_3 (\Gamma_1 - 1)^2 A A B + (\xi_2 i \omega_2 + \alpha_2) B + 2i D_1 \omega_2 B = (\omega_1^2 - \omega_2^2) + 3\alpha_3 B^2 B] - 6\beta_1 (\Gamma_1 - 1)^2 A A B - \xi_3 i \omega_2 B - 3\beta_1 B^2 B \tag{23}$$

Expressing the complex functions A and B in polar form, we have:

$$A = a e^{i\theta} \tag{24}$$

$$B = b e^{i\gamma} \tag{25}$$

$$B = be$$

2

where, a, b, ϕ and ψ are real. Substituting Eqs. (24) and (25) in Eqs. (22) and (23) and separating the real and imaginary parts, we obtain the following set of solutions:

$$a' = c_1 a - d \sin(\eta) \tag{26}$$

$$a\eta' = c_2 a + c_3 a^3 + c_4 ab^2 - d \cos(\eta) \tag{27}$$

$$b' = c_5 b \tag{28}$$

$$b\gamma' = c_6 b + c_7 b^3 + c_8 a^2 b \tag{29}$$

where

$$f = \begin{bmatrix} 1 & 1 & 3 & 3 \\ 3 & 1 & 2 \end{bmatrix}, \tag{30}$$

$$d = \dots, c_1 = [-\xi_1 + \xi_2(\Gamma_1 - 1)], c_2 = -\alpha_2 \Gamma_1, c_3 = [\alpha_1 - \alpha_3(\Gamma_1 - 1)$$

$$2\omega_1^2 \quad 2\omega_1^8 \omega_1$$

$$c_4 = -\alpha_3(\Gamma_1 - 1), c_5 = (\xi_2 \omega_2^2 \Gamma_2 - \xi_3 \tag{31}$$

$$4\omega_1^2$$

$$3 \quad 3 \quad 3 \quad 2$$

$$c_7 = -\alpha_3 \omega_2^2 \Gamma_2 + \beta_1, c_8 = -\alpha_3(\Gamma_1 - 1) \omega_2^2 \Gamma_2 +$$

$$8 \quad 8\omega_2^4$$

1

$$\beta_1 \Gamma_1 - 1)^2 \tag{32}$$

where $\Gamma_2 = 2 \omega_2^2$, $\eta = \theta - \sigma T_1$, a and θ are the amplitude and phase of the main system, $\omega_1 - \omega_2$ respectively, b and ϕ are amplitudes and phase of the absorber.

In order to obtain stationary solutions, we do $a' = b' = \eta' = \gamma' = 0$ in (26) - (29). Thus, the stationary values become solutions of an algebraic system of equations:

$$c_1 a - d \sin(\eta) = 0 \tag{33}$$

$$(c_2 - \sigma)a + c_3 a^3 - c_4 ab^2 - d \cos(\eta) = 0 \tag{34}$$

$$c_5 b = 0 \tag{35}$$

$$c_6 b + c_7 b^3 + c_8 a^2 b = 0 \tag{36}$$

Resolving the resulting algebraic equations (33) - (36) produces three possibilities for the fixed points, namely:

Case (1): $a \neq 0, b = 0$;

Case (2): $a = 0, b \neq 0$ and Case (3): $a \neq 0, b \neq 0$. in which only the first can happen.

Thus, considering $b=0$ and squaring the two sides of each of the Eqs. (33) and (34) and summing them, we obtain:

$$[(c_2 - \sigma + c_3 a^2)^2] a^2 + c_1^2 a^2 = d^2 \tag{37}$$

which is the frequency response for the system given in Fig.1.

It is worth mentioning that the values of a and η are solutions of Eqs. (33) and (34), since the case in which $b = 0$ is considered.

Figure 3 shows the variation in a and η in relation to T_1 calculated by a numerical integration of equations (33) and (34). It can be noted that, in principle a and η exhibit oscillations, but in the steady state it becomes constant.

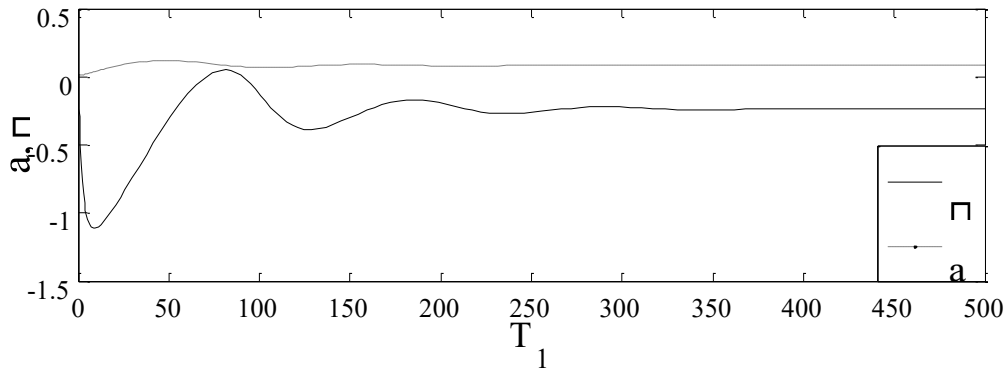


Figure 3: Variation in a and η with T_1 numerically calculated (25) and (26) to $\sigma = 0, b = 0, a(0) = 0.01$ and $\eta(0) = 0.01$.

In order to analyze the stability, we will use the method by Andronov and Vitt (see [27] and [23]). Thus, considering the first order approximate:

$$\begin{aligned} \eta a &= a_0 + a_1 \\ \eta \eta &= \eta_0 + \eta_1 \\ \eta b &= b_0 + b_1 \end{aligned} \tag{38}$$

where a_0, η_0 and b_0 are solutions of the steady state. Substituting Eq. (38) in equations (33)-(36), we have:

$$\begin{aligned} \eta a_1' &= \eta a_1 \\ \eta \eta_1' &= J \eta_1 \\ \eta b_1' &= \eta b_1 \end{aligned} \tag{39}$$

where J is the Jacobian matrix given by:

$$J = \begin{bmatrix} c_1 & -(c_2 - \sigma)a_0 - c_3a_0^3 & 0 \\ -(c_2 - \sigma) + 3c_3a_0 & c_1 & 0 \end{bmatrix} \tag{40}$$

$$\begin{bmatrix} a_0 & 0 & 0 \\ 0 & 0 & 0 \\ 0 & 0 & c_5 \end{bmatrix}$$

The eigenvalues of matrix J are given by:

$$\lambda^3 + c_9\lambda^2 + c_{10}\lambda + c_{11} = 0 \tag{41}$$

where c_9, c_{10} and c_{11} are the following constants:

$$c_9 = -2c_1 - c_5 \tag{42}$$

$$c_{10} = 3a_0^4c_3^2 + 4a_0^2c_2c_3 - 4a_0^2c_3\sigma + c_{22} - 2c_2\sigma + c_{12} + 2c_5c_1 + \sigma^2 \tag{43}$$

$$c_{11} = -3c_5a_0^4c_3^2 - 4c_5a_0^2c_2c_3 + 4c_5a_0^2c_3\sigma - c_5c_{22} + 2c_5c_2\sigma - c_5c_{12} - c_5\sigma^2 \tag{44}$$

4.1 Saddle-node bifurcation

The real parts of the eigenvalues of matrix J determines the amplitude of oscillations of the coupled system (3) and (4). Thus, if we denote by λ_{ci} the eigenvalues of matrix J, we see that equation $Real(\lambda_{ci})=0$ determines the points at which the solutions bifurcate, [28], [29]. In it, there are three real solutions between two points of vertical tangent, which are called limit point bifurcation, known in the literature as saddle-node bifurcation.

The saddle-node bifurcation is a nonlinear phenomenon and is related with a nonlinear model of a quadratic equation [30]. At the saddle-nodes, the tangency of the frequency response curve is vertical. The locations of the jumping points are obtained through differentiation of the

d^σ frequency response Eq. (37) with respect to a and considering $da_2 = 0$. Thus, the resulting expression is

$$(c_3a^2 + c_2 - \sigma)^2 + c_1^2 + 2a^2c_3(c_3a^2 + c_2 - \sigma) = 0, \tag{45}$$

in which the solution is given by:

$$\sigma_{\pm} = c_2 + 2c_3a^2 \pm \sqrt{c_3^2a^4 - c_1^2}. \tag{46}$$

From equations (46), we can obtain an interval $\sigma_- \leq \sigma \leq \sigma_+$ in which three real and positive solutions can be obtained from Eq. (37).

4.2 Stability analysis

The stability region of the frequency response curve, Eq. (37), will be determined by Routh-Rurwitz criterion. A system is considered stable if all eigenvalues of the Jacobian matrix associated with a particular point of balance have a negative real part [10]. In order to apply the Routh-Hurwitz criterion, all coefficients

and determinants of Hurwitz matrix (H) must be positive. If one of these values is negative, the Jacobian matrix has at least one eigenvalue with a positive real part, making the system unstable [7].

Thus, considering Eq. (41), matrix H is constructed:

$$H = \begin{bmatrix} c_9 & c_{11} & 0 \\ 0 & c_9 & c_{11} \\ 0 & 0 & 0 \end{bmatrix}$$

$$H = \begin{bmatrix} 1 & c_{10} & 0 \\ c_9 & 1 & c_{11} \\ 0 & c_{10} & 1 \end{bmatrix} \tag{47}$$

$$\begin{bmatrix} 0 & c_9 & c_{11} \\ c_9 & 1 & c_{11} \\ 0 & 0 & 0 \end{bmatrix}$$

Applying the Routh-Hurwitz criterion in Eq.(41), we obtain the following set of inequalities $c_9 > 0, c_{10} >$

$$0, c_{11} > 0, c_9 c_{10} - c_{11} > 0, c_9 c_{10} c_{11} - c_{11}^2 > 0. \tag{48}$$

If the expressions are in accordance with Eq. (48), then all the critical points of the system given by Eqs (26) to (29) are stable, otherwise they are unstable.

4.3 Frequency response for the system

The expression given in Eq.(37) is a nonlinear algebraic equation solved numerically using implementations in software MATLAB® and the result is shown in Fig. 4. In this figure, the frequency response curve is composed of continuous and dashed lines, which represent the stable and unstable solutions, respectively, calculated according to the Routh-Hurwitz criterion.

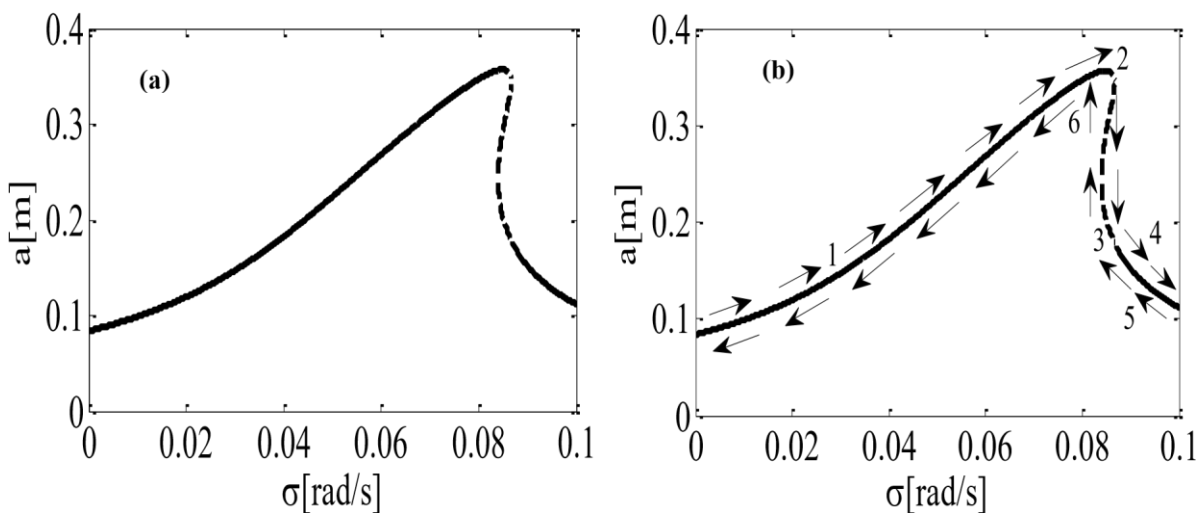


Figure 4: (a) Amplitude of the main system in case of a primary resonance with $f_0 = 0.2106N$, (b) Jump Phenomenon.

In Figure 4 (a), we note that the curve shows the jump phenomenon that is one of the outstanding characteristics of nonlinear systems. The jumping phenomenon occurs where the steady state behavior

changes dramatically due to a transition from one stable solution to another unstable solution when the tuning parameter σ is varied.

Figure 4 (b) shows the jump phenomenon. Initially, in point 1, we see that the curve of the input frequency σ is low. As the frequency σ is increased, amplitude a increases until point 2 is reached. If the frequency σ increases, then it undergoes a jump from position 2 to position 3. This part of the response is unstable (eigenvalues of the Jacobian matrix have a positive real part). In addition, a change in its amplitude and phases can be observed. When the frequency σ increases, the amplitude follows curve Section 3 towards point 4. On the other hand, in the opposite direction, there is a decrease in the values of the frequency. In this figure, the frequency response for the main system was also observed. It has a maximum value of peak amplitude in $a_{max} = 0.3568m$ that occurs when $\sigma = 0.0850 \text{ rad /s}$ and presents an unstable region in the interval $0.08399 \leq \sigma \leq 0.08669$, as shown in the eigenvalues listed in Table 2. Is worth mentioning that the stability region was obtained applying the Routh Hurwitz criterion as described above.

Table 2: Eigenvalues of the system with nonlinear absorber in force $f_0 = 0.2106N$.

σ	λ_1	λ_2	λ_3
0	-0.0137 + 0.05872i	-0.0137 - 0.05872i	-0.045
0.08	-0.0137 + 0.014051i	-0.0137 - 0.014051i	-0.045
0.08398	-0.0137 - 0.0073204i	-0.0137 + 0.0073204i	-0.045
0.08399	-0.0137 + 0.007265i	-0.0137 - 0.007265i	-0.045
	-0.028148	0.00062373	
0.08669	-0.0137 + 0.01465 - 0.026818 i	-0.0137 - 0.00070583 - 0.01465 i	-0.045
	-0.026881	-0.00064263	
0.08671	-0.0137 + 0.01472 - 0.028113 i	i - 0.01370.00058928 - 0.01472 i	-0.045
0.09	-0.0137 + 0.023129i	-0.0137 - 0.023129i	-0.045
0.1	-0.0137 + 0.03856i	-0.0137 - 0.03856i	-0.045

5 Numerical results and discussion

To study, numerically, the behavior of the main system and the absorber, the Runge-Kutta fourth-order method was applied to Eqs. (3) and (4) with implementations in software Matlab®, according to [31]. In order to do this, we rewrite Eqs. (3) and (4) as a system of first order differential equations, given by:

$$\dot{x}_l = y_l$$

$$m_1 \ddot{y}_1 = -k_{12} x_1 - k_{11} (x_1^3) - k_{11} y_1 + k_{12} x_2$$

$$m_1 \ddot{x}_1 + k_{13} (x_2 - x_1)^3 - k_{12} (y_1 - y_2) + k_{11} \cos(\omega t)$$

$$\tag{49}$$

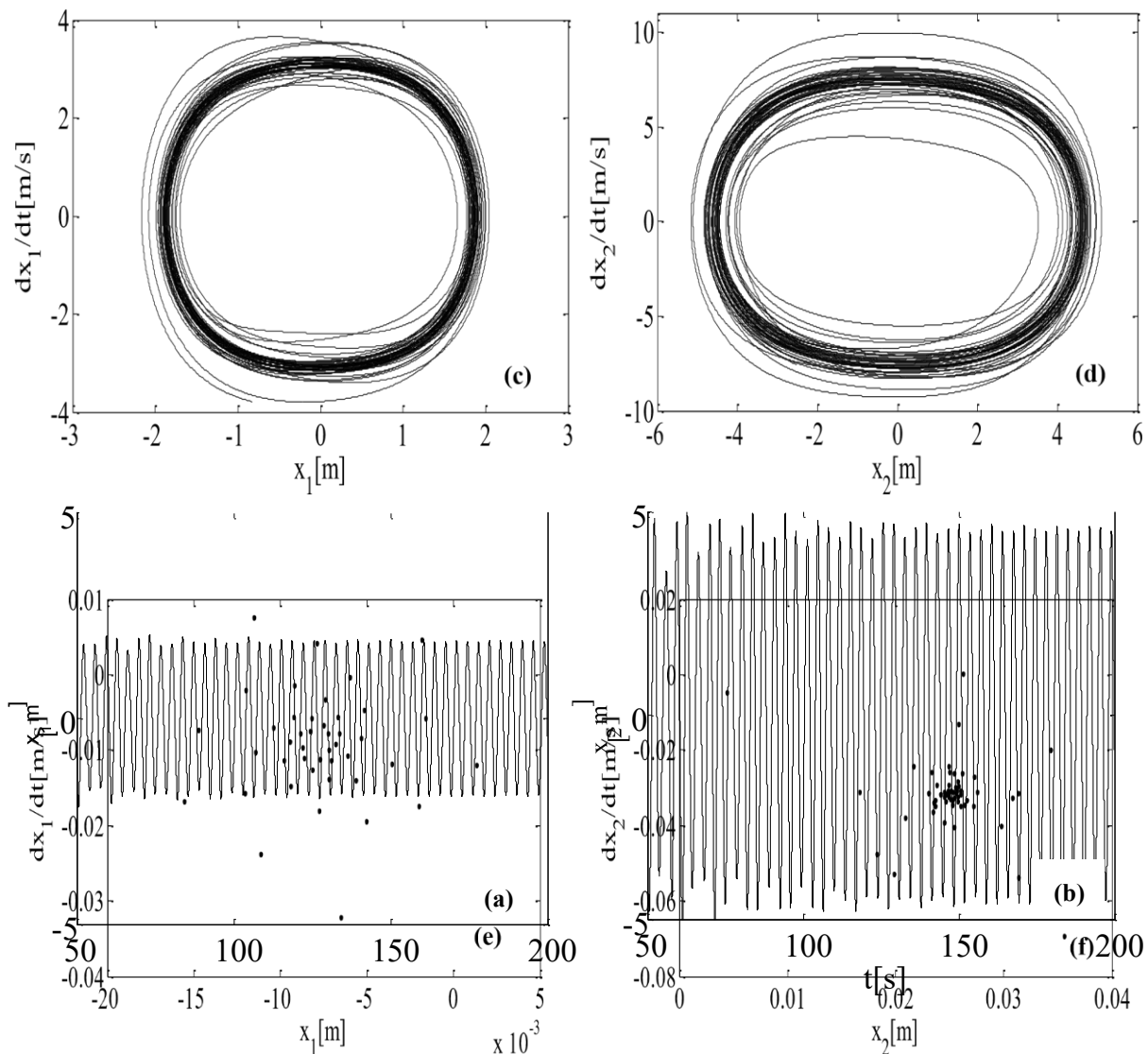
$$m_2 \ddot{x}_2 = y_2$$

$$m_2 \ddot{y}_2 = -k_{22} (x_2 - x_1) - k_{21} (x_2 - x_1)^3$$

$$m_2 \ddot{y}_2 - k_{23} (y_2 - y_1)$$

The responses in the time domain, phase planes and Poincaré sections of the main system and absorber, varying the parameter of amplitude force are shown in Figures 5 - 7. In this study, we considered the case of primary resonance. The simulations were performed eliminating the initial transient part and the values of system parameters are listed in Table 1.

Figure 5: (a) – (b) Response, (c) – (d) phase plan and (e) – (f) sections of Poincaré of the main system



and absorber, respectively, in primary resonance $\Omega \approx 1$ and $f = 0.02$.

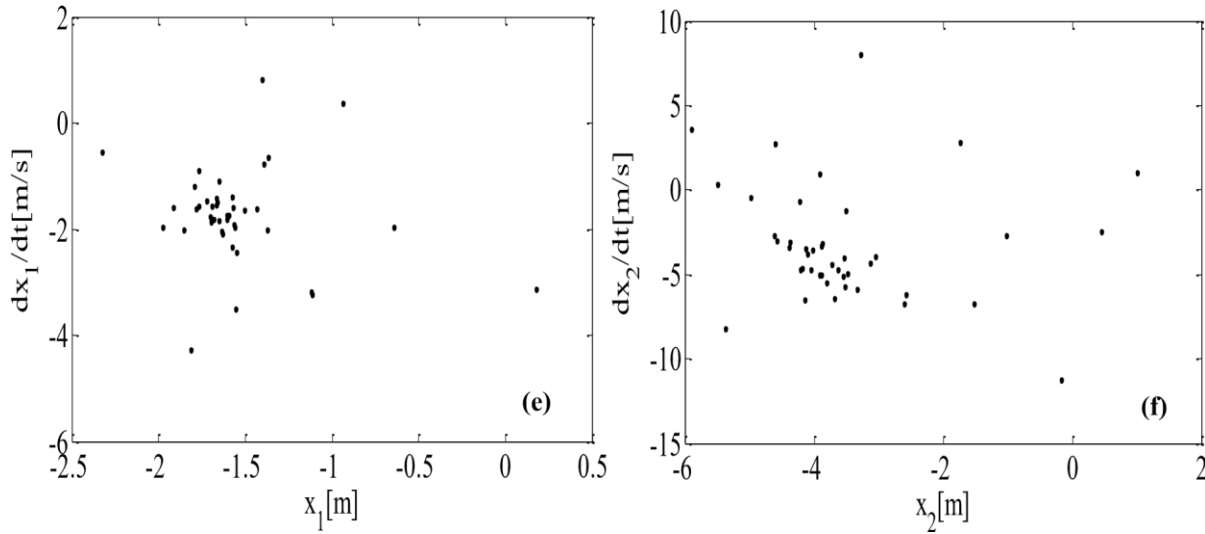


Figure 6. (a) – (b) Response, (c) – (d) phase plan and (e) – (f) Poincaré section of the main and absorber system, respectively, in primary resonance $\Omega \approx 1$ and $f = 5$.

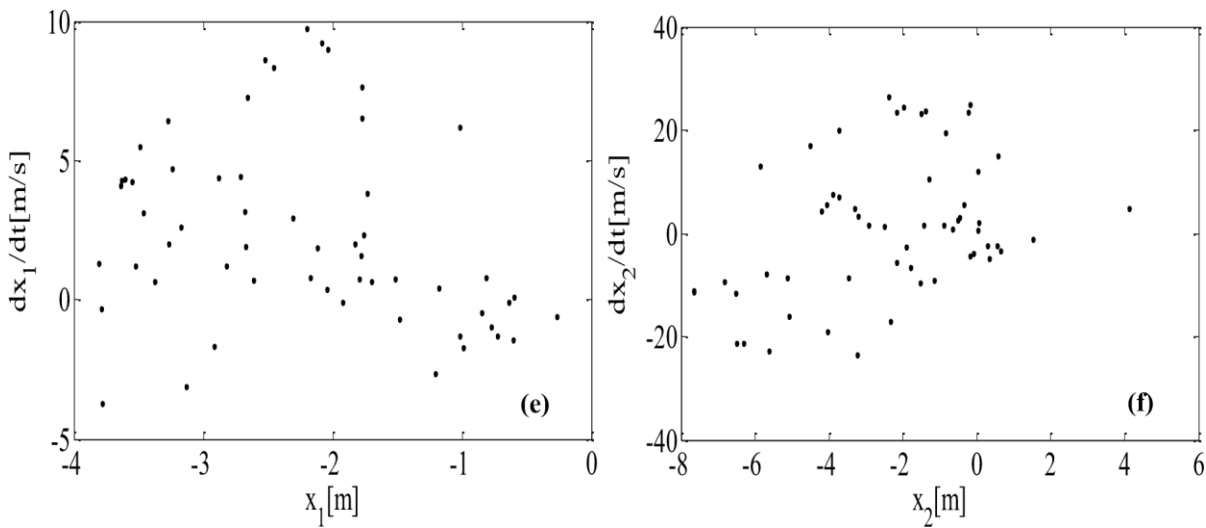
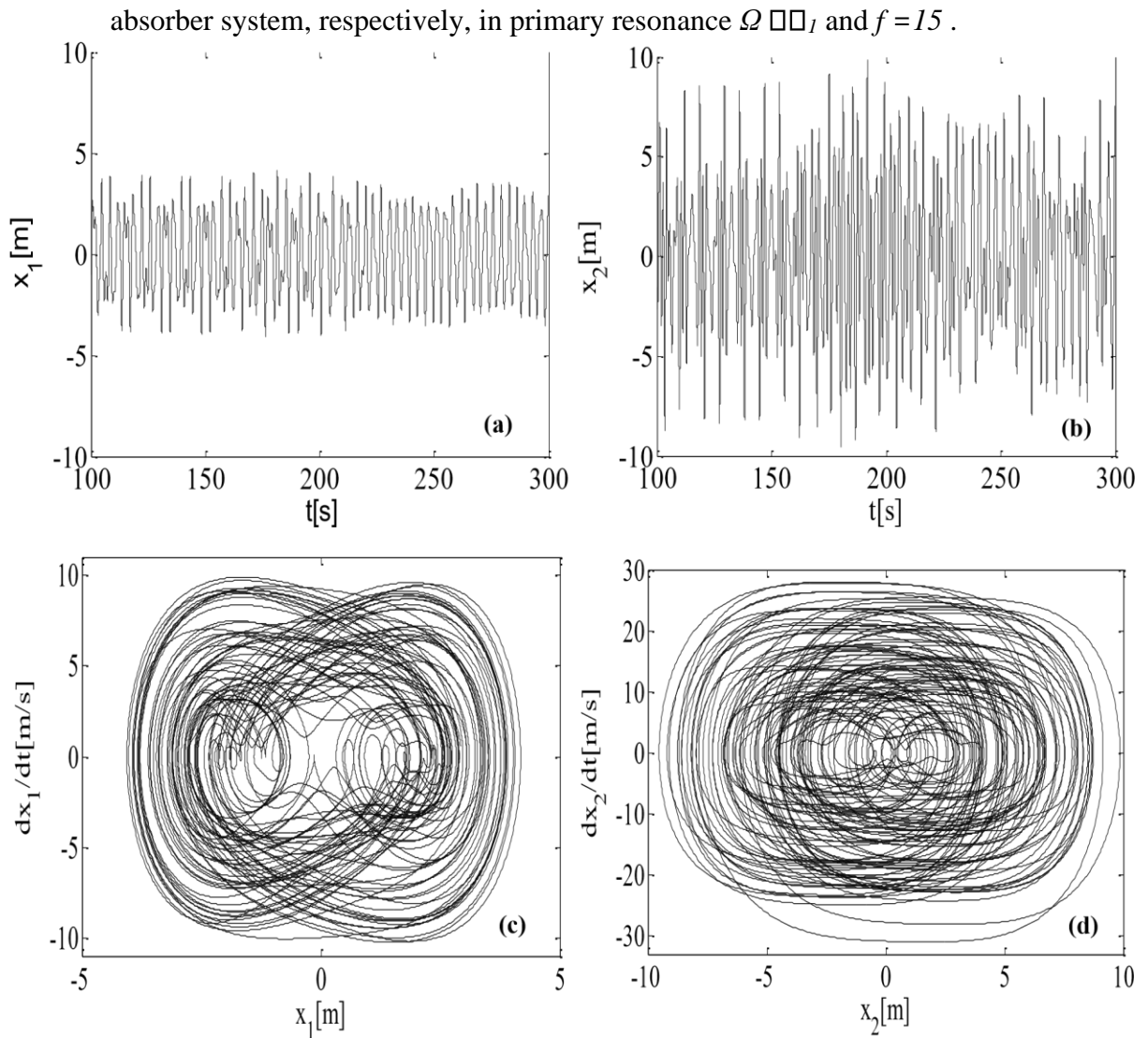


Figure 7: (a) – (b) Response, (c) – (d) phase plan and (e) – (f) Poincaré section of both the main and



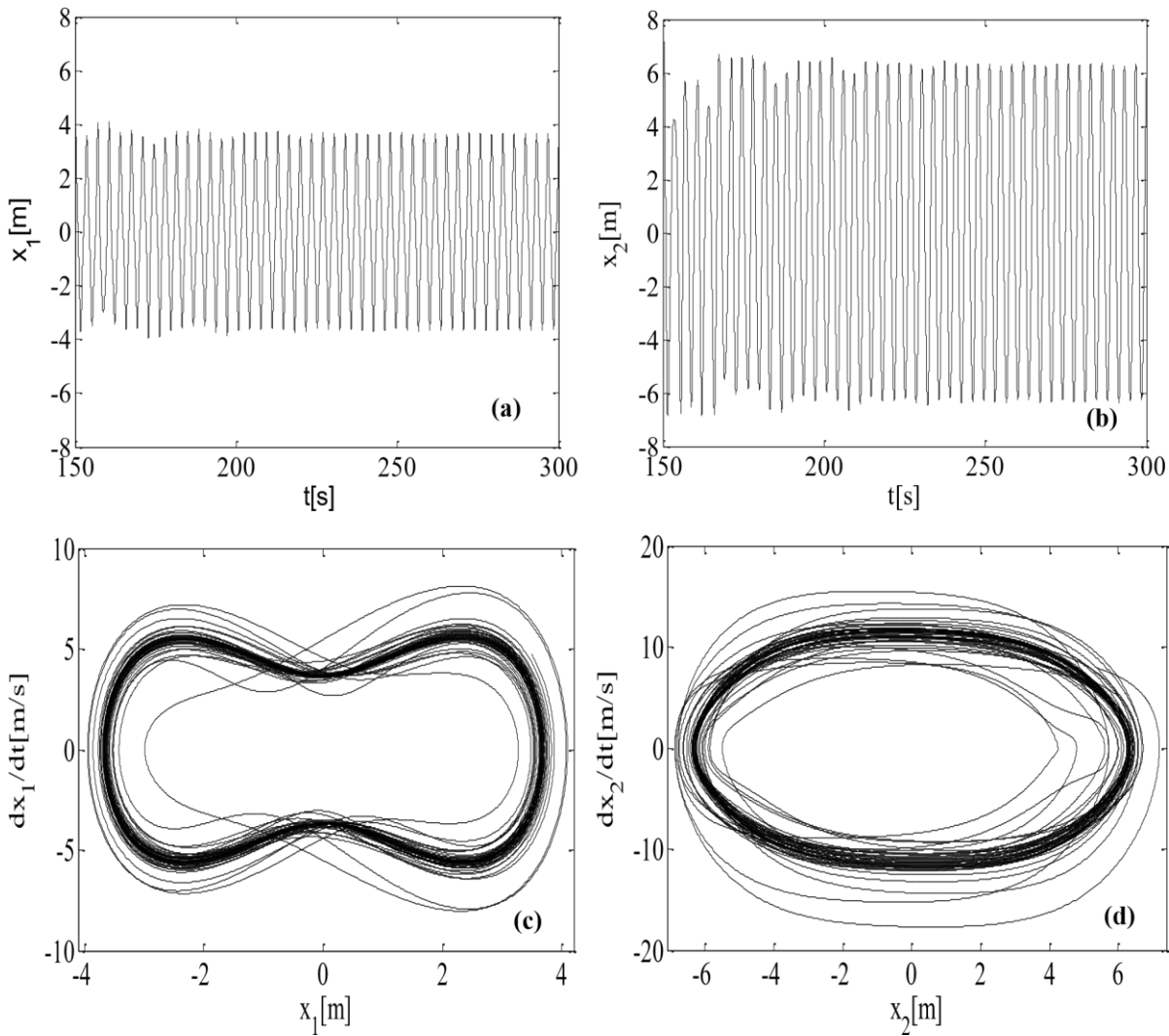
In Figure 5, when $f = 0.02$, note that the graphics of evolution in the time domain, represented by (a) and (b), in Figure 5 correspond to the behavior of both the main and secondary system (absorber), respectively, which exhibit low-amplitude oscillations around the steady solution. They are initially irregular, and after a period of time, become regular. It can be observed that the closed curves in the phase pictures, Figure 5 (c) and (d), for both the main system and the absorber system, are characteristic of periodic behavior. As a result of this, the Poincaré sections display points closer to each other, as can be seen in Figure 6 (e) and (f):

For $f = 5$, Figure 6 (a) and (b), we note a considerable increase in the response amplitudes of both the main system and the absorber. In the phase picture, given by Figure 6 (c) and (d), it can be observed that an increase in the oscillation of the system occurs. However, both systems continue to show considerable stable behavior, as shown in the Poincaré sections, Figure 6 (e) and (f).

In Fig. 7 (a) and (b), the responses in the time domain for $f = 15$ are observed. In these responses, both the main system and the absorber have irregular oscillations, that is, there is a well-defined period. On the other hand, Figure 7 (c) and 7 (d) show evidence of chaotic behavior. This behavior is obtained by analyzing the

Poincaré section of both main and secondary systems (absorber), according to Figure 7 (e) and (f), respectively, as their points are irregularly scattered on the phase plane.

Fig.8 shows the results obtained for the main system and absorber, for $f = 25$. When compared with $f = 15$ in Figure 7, the behavior of the complete system in the case $f=25$ (Figure 8), is more stable, but still exhibits chaotic behavior. Figure 9 shows responses of the system (both main and absorber system) for $f = 30$. The system presents chaotic behavior showing an increase in irregular variation (c) and (d). Fig. 9 (e) and (f) for the main and secondary (absorber) systems also show a large number of scattered points in the plane.



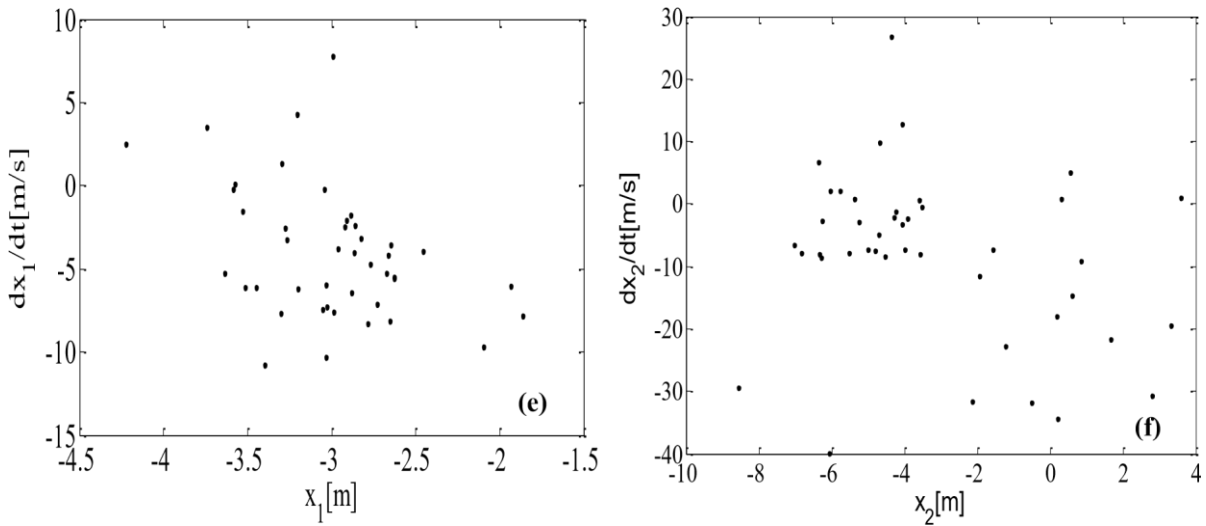
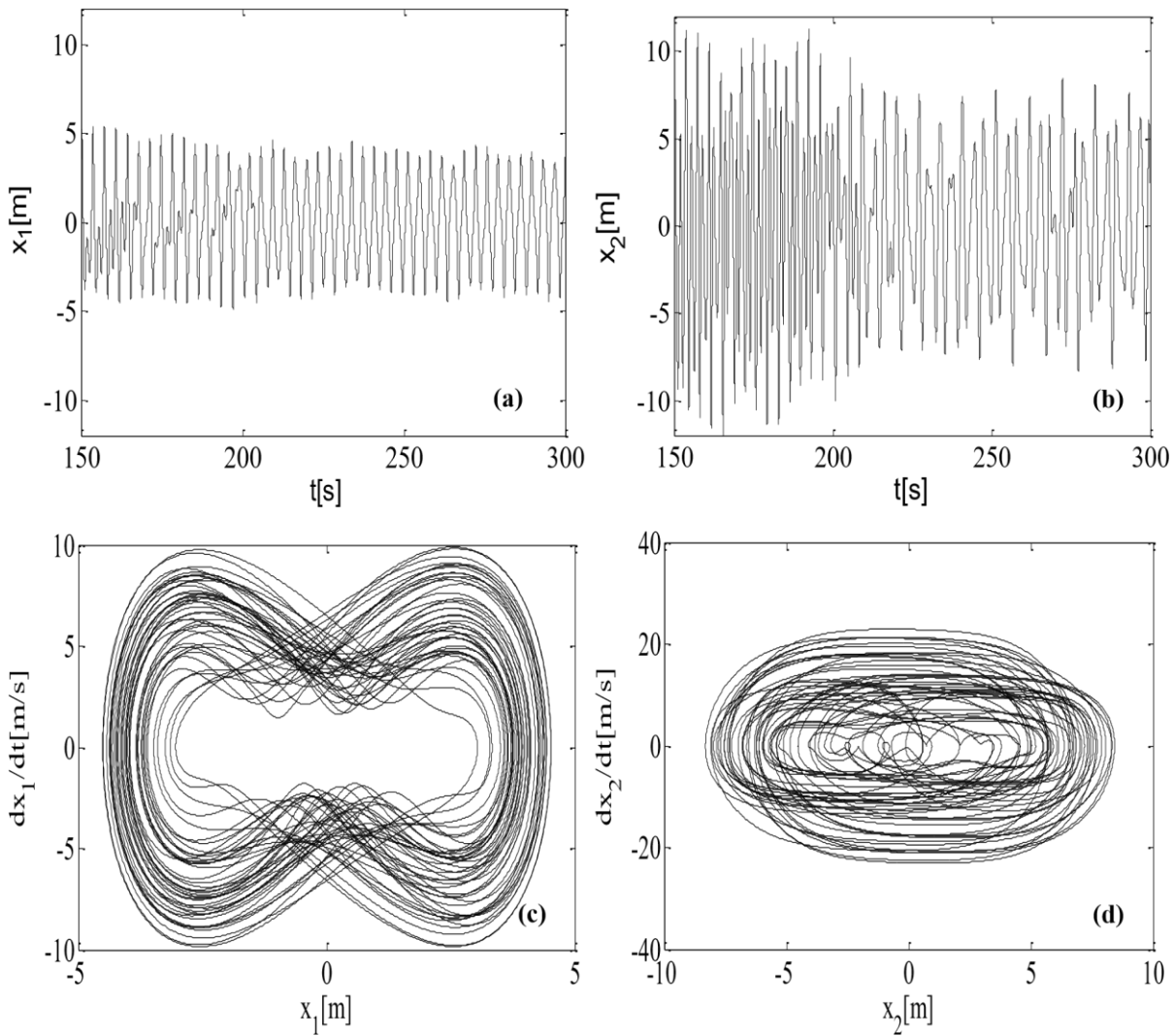


Figure 8: (a) – (b) Response, (c) – (d) phase plan and (e) – (f) Poincaré section of both the main and absorber system respectively, in primary resonance $\Omega \approx \omega_1$ and $f = 25$.



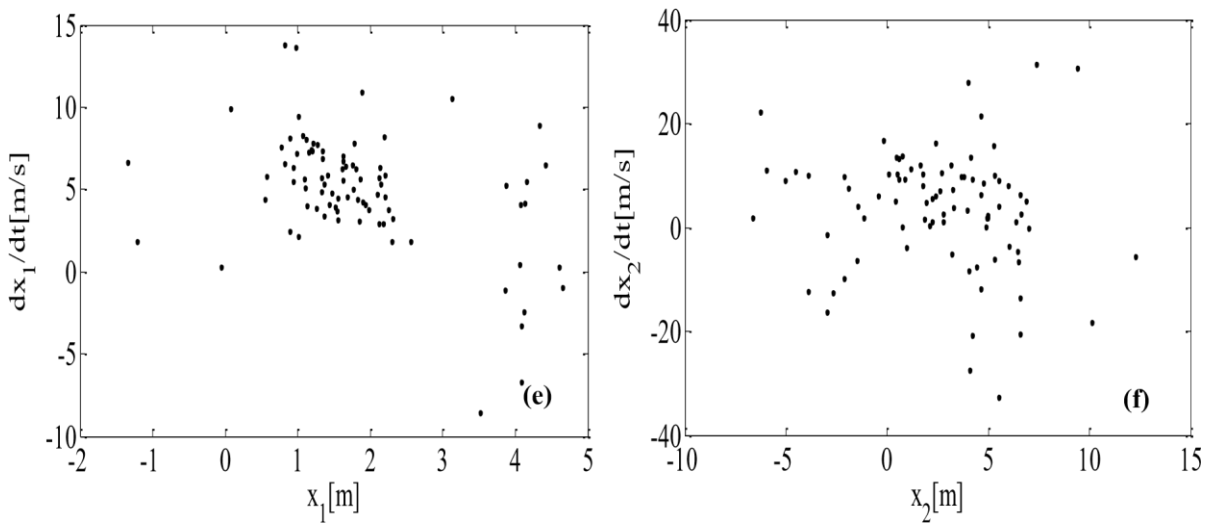


Figure 9: (a) – (b) Response, (c) – (d) phase plan and (e) – (f) Poincaré section for the main system and absorber, respectively, in primary resonance $\Omega \approx \omega_1$ and $f = 30$.

5.1 Lyapunov Exponent

In this section, we apply the methods of Lyapunov exponents to analyze the existence of both periodic and chaotic orbits, [23]. As we can see from system (Eq. 50), the set of equations form a nonautonomous system. In order to transform it into an autonomous one, we introduce the new variable $z = t$, obtained from the autonomous system below,

$$\dot{x}_1 = y_1$$

$$\dot{y}_1 = -\omega_1^2 x_1 - \omega_1(x_1^3) - \omega_1 y_1 + \omega_2 x_2 + \omega_3(x_2 - x_1)^3 - \omega_2(y_1 - y_2) + f \cos(\omega_1 z)$$

□

$$\dot{x}_2 = y_2 \tag{50}$$

$$\dot{y}_2 = -\omega_2^2(x_2 - x_1) - \omega_2(x_2 - x_1)^3 - \omega_2^3(y_2 - y_1)$$

$$\dot{z} = 1$$

From the system of equations (50), we perform the calculation of Lyapunov exponents, using a computer program implemented in the Matlab[®] software. The results are shown in Figure 10 (a) – (f) for the following values $f = 0.02$, (b) $f = 5$, (c) $f = 15$, (d) $f = 25$, (e) $f = 30$ and (f) $f = 40$, respectively. The parameter values used in the simulations are listed in Table 1, and the initial conditions are considered zero. It is worth mentioning that the first two hundred iterations were eliminated to better interpret these exponents.

We can see from Figures 10 (a) and (b) for $f = 0.02$ and $f = 5$, respectively, that the system has periodic behavior, since most of their exponents are null, indicating that the paths do not diverge. In the case where

$f = 15$, $f = 25$, $f = 30$ e $f = 40$, Figure 10 (c), (d), (e) and (f), respectively, shows that the solutions of the system exhibit chaotic behavior, i.e., it presented Lyapunov positive exponents. In these cases, there is a separation of paths when they migrate to a certain direction with a passage of time, featuring chaos.

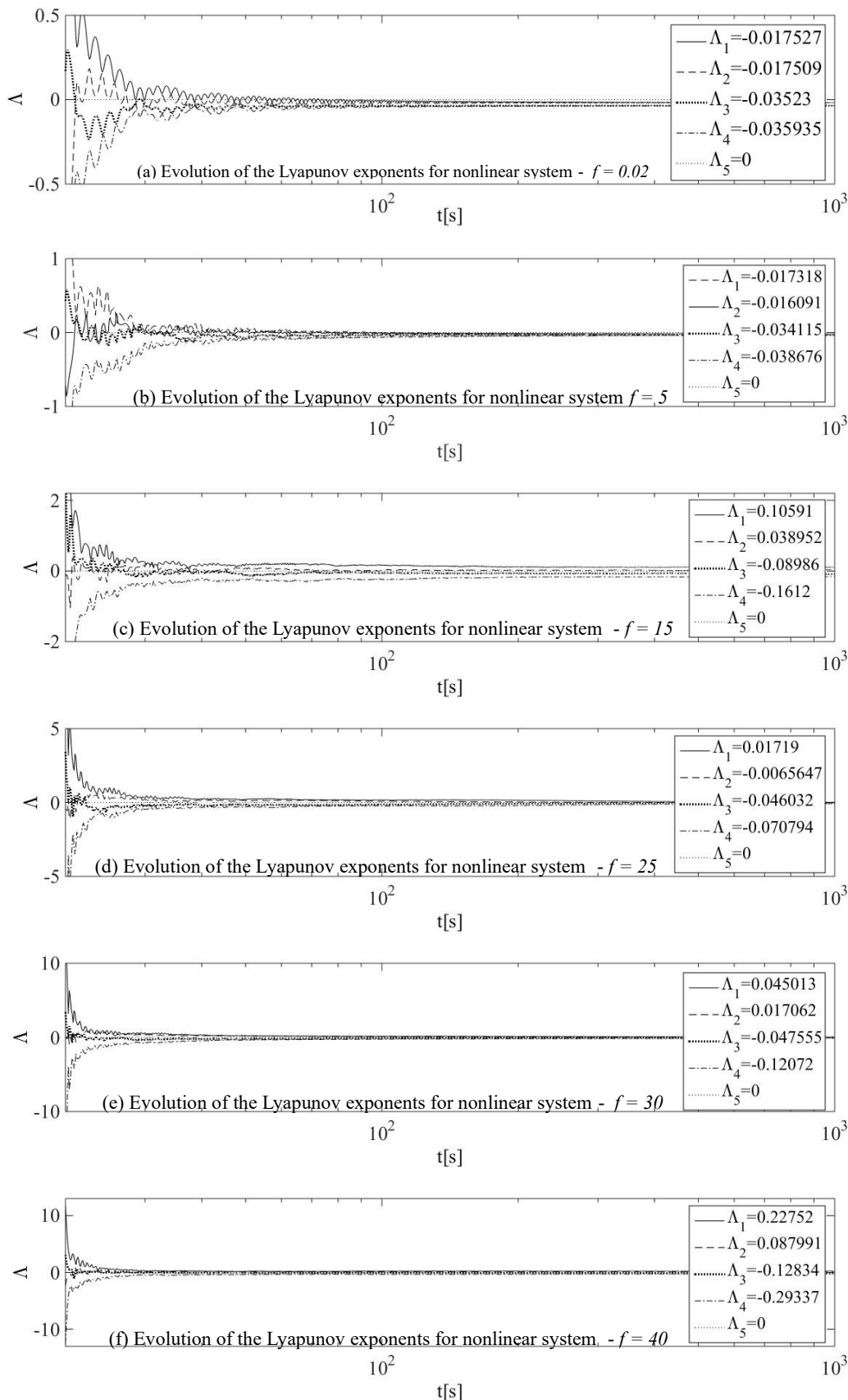


Figure 10. Evolution of the Lyapunov exponents of the system with nonlinear absorber ($f = 0.02, 5, 15, 25, 30, 40$)

The responses in the time domain phase Portrait phase and the Poincaré sections showed the presence of chaotic behavior in the dynamics system, verified by the analysis of the signs of Exponents Lyapunov, as presented in Table 3.

Table 3 – Signs of Lyapunov Exponents

Driving amplitude f	Signs of Lyapunov Exponents			
0.02	-	-	-	-
5	-	-	-	-
15	+	+	-	-
25	+	-	-	-
30	+	+	-	-
40	+	+	-	-

Figure 11 shows the global behavior of the system (Eq.49). As we can see the system undergoes bifurcations [32] for frequency values between (10 – 20), (28 – 32), (36 – 50) for both the main and secondary system.

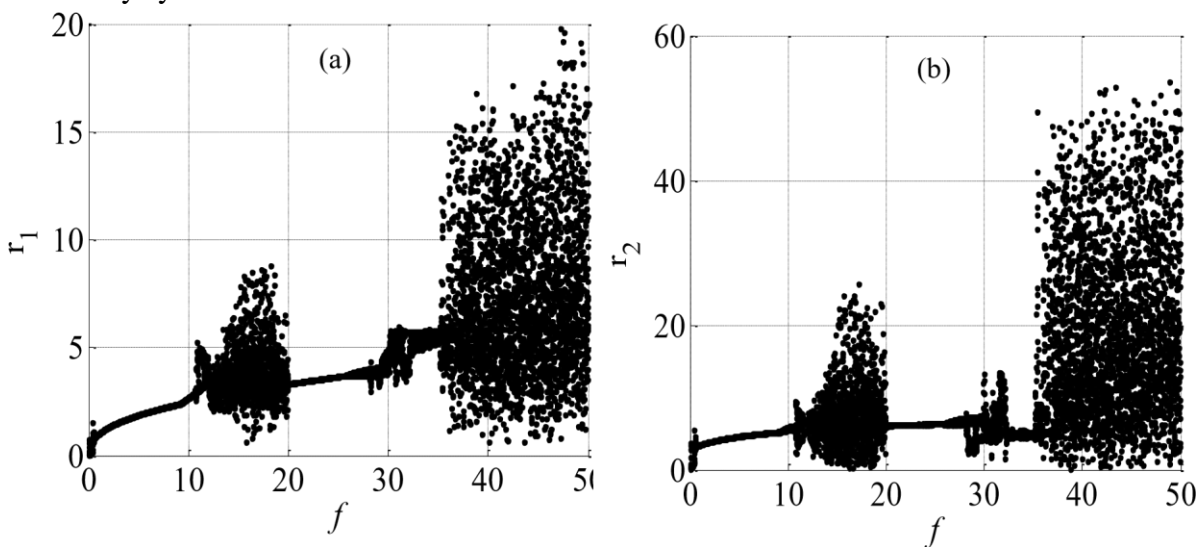


Figure 11: A bifurcation diagram for (a) main system and (b) absorber

In the bifurcation diagram for the primary system (Figure 11 (a)), it can be observed that for $0 < f < 10.5$, there are regions where parameter f is associated with a finite number of points. It can be observed in this figure that for f values given by $10.5 < f < 20$, the system is modified to a regime of unstable solutions and in this case it can be seen that there is a bifurcation of the solution. However, for the interval $20 < f < 26$, the system exhibits a stable behavior, but again the system presents a region of solution instabilities by increasing the magnitude of the force in the region that comprises the interval $26 < f < 50$.

Figure 11 (b) shows that the absorber has a very similar behavior to the main system, which values $0 < f < 9$ and $20 < f < 26$ the parameter f is associated with a finite number of points, and for $9 < f < 20$ and $26 < f < 50$ the regions have shown clouds of points, indicating where the chaotic behavior occurs.

6 Conclusion

In this paper, we investigated the behavior of a nonlinear system with a nonlinear absorber in primary resonance, discussing the characteristics of the theory of mechanical vibration as a nonlinear system. As shown in the numerical simulations, it can be observed that the Multiple Scale Method satisfactorily describes the behavior of the coupled system.

For the primary resonance case, the amplitude of frequency response of the main system, with force $f_0 = 0.2106N$, corresponds to a curve which exhibits the jumping phenomena, which consists of a curve where in one direction the system has stability and in another the system exhibits instability behavior. The region of stability of the solutions is determined by Routh-Rurwitz criterion, which is efficient analysis from both stability and instability behavior.

We pointed out that the interval of $0.08399 \leq \sigma \leq 0.08669$ comprises a region in which the Routh-Hurwitz criterion is not satisfied and therefore, it is called an unstable region. This is due to the fact that the one of eigenvalues of the equations has a positive real part.

Numerical results are presented in different ways: time domain responses, in phase portrait form, Poincare sections and Lyapunov exponents. The computational simulations were performed through computer programs in MATLAB® software. The time domain responses show trajectories, initially irregular, becoming regular when time goes to infinity. Analyzing the phase portraits, it is evident that the system presents an unstable (chaotic) irregular behavior. The Poincare sections have irregular oscillations with a number of periods, which are not defined.

The stability of the system in question is verified by means of two important criteria of nonlinear dynamics, namely Routh-Hurwitz criterion and an analysis of Lyapunov exponents. The theory of the Lyapunov exponent is also a useful tool in the stability analysis, since the simulations showed the existence of a positive exponent, ensuring the existence of chaos. In addition, the simulations indicated the existence of a zero exponent, which according to theory, ensures the existence of a periodic response. Therefore, both Routh-Hurwitz criterion and Lyapunov exponents provided good results regarding the stability of dynamic systems.

Acknowledgements

The authors are grateful to the Goiás State Agency FAPEG for the financial support to their research activities, the Coordination for the Improvement of Higher Education Personnel – CAPES and CNPq (grant #439126/2018–5) for the continued support to their research work.

7 References

- [1] Sayed, M.; Hamed, Y. S., Amer, Y. A.: Vibration Reduction and Stability of Non-Linear System Subjected to External and Parametric Excitation Forces under a Non-Linear Absorber. *IJCMS: International Journal of Contemporary Mathematical Sciences*, 22, 1051– 1070, (2011).
- [2] Rade, D. A. and Steffen, V. Jr.: Dynamic Vibration Absorber. *Encyclopedia of Vibration*, Academic Press, ISBN 0-12-227085-1, 9-26 (2011).
- [3] Koronev, B. G., Reznikov, L. M.: *Dynamic Vibration Absorbers: Theory and Technical Applications*. John Wiley and Sons Ltd., Chichester, UK, (1993).
- [4] Borges, R. A., de Lima A.M.G., Steffen Jr, V.: Robust optimal design of a nonlinear dynamic vibration absorber combining sensitivity analysis, *Shock and Vibration* 17, 507-520, (2010).
- [5] Awrejcewicz, J., Krysko, A. V., Zagniboroda, N. A., Dobriyan, V. V., Krysko, V. A.: On the general theory of chaotic dynamics of flexible curvilinear Euler–Bernoulli beams, *Nonlinear Dynamics* 79,11 – 79, (2015).
- [6] Thiery, F., Aidanpää, J. O.: Nonlinear vibrations of a misaligned bladed Jeffcott rotor, *Nonlinear Dynamics* 86, 1807 – 1821, (2016).
- [7] Thomsen, J. J. *Vibration and Stability Advanced Theory, Analysis, and Tools*. SpringerVerlag, 2nd Edition, (2003).
- [8] Awrejcewicz, J., Krysko, V. A.: *Chaos in Structural Mechanics*, Springer-Verlag Berlin Heidelberg, (2008).
- [9] Vadasz, P., Equivalent initial conditions for compatibility between analytical and computational solutions of convection in porous media, *International Journal of Non-Linear Mechanics* 36, 197-208 (2001).
- [10] Nayfeh, A, H.: *Perturbation Methods*. John Wiley and Sons, New York, (2004).
- [11] Rabelo M. Silva, L., Borges, R.A., Gonçalves, R. Henrique, M., Computational and Numerical Analysis of a Nonlinear Mechanical System with Bounded Delay, *International Journal of Non-Linear Mechanics* 91, (2018), 36-57.
- [12] Lee, K. H., Han, H. S., Park, S., Bifurcation analysis of coupled lateral/torsional vibrations of rotor systems, *Journal Sound and Vibration* 386, (2017), 372 – 389.
- [13] Srinil N and Zanganeh H 2012 Modelling of coupled cross-flow/in-line vortex-induced vibrations using double Duffing and van der Pol oscillators, *Ocean Engineering.*, 53, 83-97 [14] Nayfeh, A. H., Balachandran, Experimental Investigation of Resonantly Forced Oscillations of a Two-Degree-of-Freedom Structure, *International Journal of Non-Linear Mechanics* 25, 199-209, (1990).

- [15] Norouzi H., Younesian D., Chaotic vibrations of beams on nonlinear elastic foundations subjected to reciprocating loads, 69, 121-128, (2015).
- [16] (zhang) Peng, Z. K., Meng, G., Lang, Z. Q., Zhang, W. M., Chu, F. L., Study of the effects of a cubic nonlinear damping on vibrations isolations using harmonic balance method. *International Journal of Non-Linear Mechanics*, 47, 1073-1080, (2012).
- [17] Zhua, Zhengb and Fu (2004) - - ZHUA; ZHENG B and FU: Analysis of Non-Linear Dynamics of a Two-Degree-of-Freedom Vibration System with Non-Linear Damping and NonLinear Spring. *Journal of Sound and Vibration*, Vol. 271, n. 1-2, 15 – 24 (2004).
- [18] J.J. Lou, Q.W. He, S.J. Zhu, Chaos in the softening Duffing system under multi-frequency periodic forces, *Applied Math. Mech.* 25 (12) (2004), 1421–1427.
- [19] M.H. Ghayesh, Stability characteristics of an axially accelerating string supported by an elastic foundation, *Mech. Mach. Theory* 44 (10) (2009) 1964–1979.
- [20] Kevorkian, J. K., Cole, J. D., *Multiple Scale and Singular Perturbation Methods*, Springer, (1996).
- [21] Burden, R. L., Faires, J. D., *Numerical Analysis*, Brooks/Cole, Cengage Learning, Ninth Edition, (2011).
- [22] Borges, R. A.; Lobato, F S. ; Steffen, V. . Application of Three Bioinspired Optimization Methods for the Design of a Nonlinear Mechanical System. *Mathematical Problems in Engineering (Print)*, v. 2013, p. 1-12, 2013.
- [23] Nayfeh, A., Mook, D., Marshall, L., Non-linear Coupling of Pitch and Roll Modes in Ship Motions, *J. Hydronautic* 7,145-152, (1973).
- [24] Kahn, P.B., *Mathematical Methods for Scientists and Engineers: Linear and Nonlinear Systems*, Jphn Wiley & Sons, New York, (2004).
- [25] Nayfeh, A.H., Balachandran, B., *Applied Nonlinear Dynamics: Analytical, Computation and Experimental Methods*. John Wiley and Sons, N.Y., (1995).
- [26] Batista, M., On stability of elastic rod planar equilibrium configurations, *International Journal of Solids and Structures* 72,144-152, (2015).
- [27] Saberi, L., Nahvi, H., Vibration Analysis of a Nonlinear System with a Nonlinear Absorber under the Primary and Super-harmonic Resonances, *International Journal of Engineering*, vol. 27, no. 3, 499-508, (2014).
- [28] Elnaggar, A.M.; and Khalil, K. M.: The Response of Nonlinear Controlled System under an External Excitation via Time Delay State Feedback. *Journal of King Saud University Engineering Sciences*. Online publication, (2014).
- [29] Chen G., Hill D. J., Yu X., *Bifurcation Control – Theory and Applications*, Springer, (2003).
- [30] Feng, Z. C., Sethna P. R., Global bifurcation and chaos in parametrically forced system with one-one resonance, *Dynamics and Stability of Systems*, 5, 201-225, (1990).
- [31] Yang, W. Y., CAO, W.; CHUNG, T. S. and MORRIS, J. (2005): *Applied Numerical Methods Using Matlab®*. John Wiley and Sons, Inc., Hoboken NJ.
- [32] Lynch, S. *Dynamical Systems with Applications using MATLAB*. Manchester: Birkhäuser Science, 2014.